SspB delivery of substrates for ClpXP proteolysis probed by the design of improved degradation tags

Greg L. Hersch*, Tania A. Baker*†, and Robert T. Sauer*‡

*Department of Biology and †Howard Hughes Medical Institute, Massachusetts Institute of Technology, Cambridge, MA 02139

Contributed by Robert T. Sauer, July 1, 2004

The ssrA-degradation tag sequence contains contiguous binding sites for the SspB adaptor and the ClpX component of the ClpXP protease. Although SspB normally enhances ClpXP degradation of ssrA-tagged substrates, it inhibits proteolysis under conditions that prevent tethering to ClpX. By increasing the spacing between the protease and adaptor-binding determinants in the ssrA tag, substrates were obtained that displayed improved SspB-mediated binding to and degradation by ClpXP. These extended-tag substrates also showed significantly reduced conditional inhibition but bound SspB normally. Both wild-type and mutant tags showed highly dynamic SspB interactions. Together, these results strongly support delivery models in which SspB and ClpX bind concurrently to the ssrA tag, but also suggest that clashes between SspB and ClpX weaken simultaneous binding. During substrate delivery, this signal masking is overcome by tethering SspB to ClpX, which ensures local concentrations high enough to drive tag engagement. This obstruct-then-stimulate mechanism may have evolved to allow additional levels of regulation and could be a common trait of adaptor-mediated protein degradation.

energy-dependent degradation | degradation specificity | degradation signals | compartmental protease | adaptor proteins

Proteases destroy other proteins. As a consequence, precise and regulated substrate selection is critical in all cells. In organisms from bacteria to humans, ATP-dependent proteases, consisting of at least one AAA+ family ATPase and a compartmental peptidase, are the major machines of cytoplasmic protein destruction (1–4). Substrate choice for these proteases is mediated by the ATPase and frequently by additional adaptor or delivery proteins (5–10). Adaptor proteins can also modulate substrate selection by AAA+ ATPases that function independent of proteases to dismantle macromolecular complexes and resolubilize aggregates (8).

The ClpXP-SspB system is a paradigm for energy-dependent degradation and adaptor-mediated target recognition (6, 11–18). Ring hexamers of the ClpX ATPase recognize protein substrates, unfold these molecules, and translocate the denatured polypeptides through a central pore, and into ClpP for degradation (1, 19–21). Processing of a single substrate can require hundreds of cycles of ATP hydrolysis and conformational change in the ClpXP machine (22–24). ClpX binds degradation tags in substrates. For example, the ssrA tag, a peptide added to the C terminus of nascent polypeptides on stalled bacterial ribosomes, targets proteins to ClpXP or ClpAP, a related AAA+ protease (25, 26). The SspB adaptor also binds to the ssrA tags of substrates, lowering K_m and enhancing substrate degradation by ClpXP, but inhibiting proteolysis by ClpAP (6, 11). An SspB dimer brings two ssrA-tagged substrates and a ClpX hexamer together in a delivery complex that is more stable than the binary enzyme–substrate complex (12, 14, 16).

Three distinct sets of protein–peptide interactions link ClpX, SspB, and the ssrA tags of substrates (11, 13–18): (*i*) ClpX binds C-terminal residues of the ssrA tag; (*ii*) the substrate-binding domain (SBD) of SspB contacts N-terminal residues in the tag (Fig. 1A); and (*iii*) an XB peptide motif at the C terminus of SspB binds the N-terminal domain of ClpX, mediating flexible tethering of these molecules. If the XB tethering motifs are removed or their binding sites on ClpX are blocked by XB peptide or other adaptors, then SspB binding inhibits ClpXP degradation of ssrA-tagged substrates, instead of enhancing this reaction (16). One attractive model for this conditional inhibition involves the close spacing of binding determinants in the ssrA tag. Because the tag residues that bind ClpX and SspB are very close (11, 13, 14), concurrent binding could result in modest steric or electrostatic clashes between ClpX and SspB (Fig. 1*B*). Such clashes would weaken binding and thus inhibit degradation of SspB-bound substrates in the absence of the tethering interactions. In tethered delivery complexes, by contrast, the high local concentration of the ssrA tag and ClpX could drive tag engagement despite the clashes. Alternatively, conditional inhibition could arise because breaking the protein–peptide interactions between SspB and the ssrA tag creates a kinetic barrier to degradation in a manner that is overcome in tethered but not in nontethered complexes with ClpX.

In the model of Fig. 1*B*, a clash occurs between SspB and ClpX because their binding sites in the ssrA tag are too close. This model predicts that the inhibitory clash could be diminished or relieved by moving these binding sites farther apart in the tag, as shown in Fig. 1*C*. To probe the mechanism of SspB delivery, we therefore constructed and tested the degradation properties of substrates with extended-spacing ssrA tags. Substrates bearing these mutant tags displayed improved SspB-mediated ClpXP degradation and significantly reduced conditional SspB inhibition. We find that interactions between the ssrA tag and SspB are highly dynamic and do not create a major kinetic barrier to degradation. These results support a "direct-handoff" model, in which SspB and ClpX bind simultaneously but with clashes to the wild-type ssrA tag (Fig. 1*B*). Hence, SspB binding changes the ssrA tag from a strong to a weak degradation signal but also functions to overcome this weakened binding by tethering the substrate to ClpX. The improved performance of the mutant ssrA tags in promoting SspB-mediated degradation shows that this tag-masking mechanism is not an obligate feature of the activation mechanism. Tag masking may have evolved to allow the SspB adaptor to function either as an enhancer or as an inhibitor of ssrA-tagged substrate degradation. The biological function of SspB may therefore depend on cellular conditions and the menu or abundance of competing ClpXP substrates and adaptor proteins.

Materials and Methods

Solutions. PD buffer contains 25 mM Hepes-KOH (pH 7.6), 5 mM KCl, 5 mM $MgCl_2$, 0.032% Nonidet P-40, and 10% glycerol. ATP regeneration mix consists of 16 mM creatine phosphate, 0.32 mg/ml creatine kinase, and 5 mM ATP. Buffer A contains 10 mM Tris·HCl (pH 7.6) and 50 mM KCl.

Abbreviation: SBD, substrate-binding domain.

‡To whom correspondence should be addressed. E-mail: bobsauer@mit.edu.

www.pnas.org/cgi/doi/10.1073/pnas.0404733101

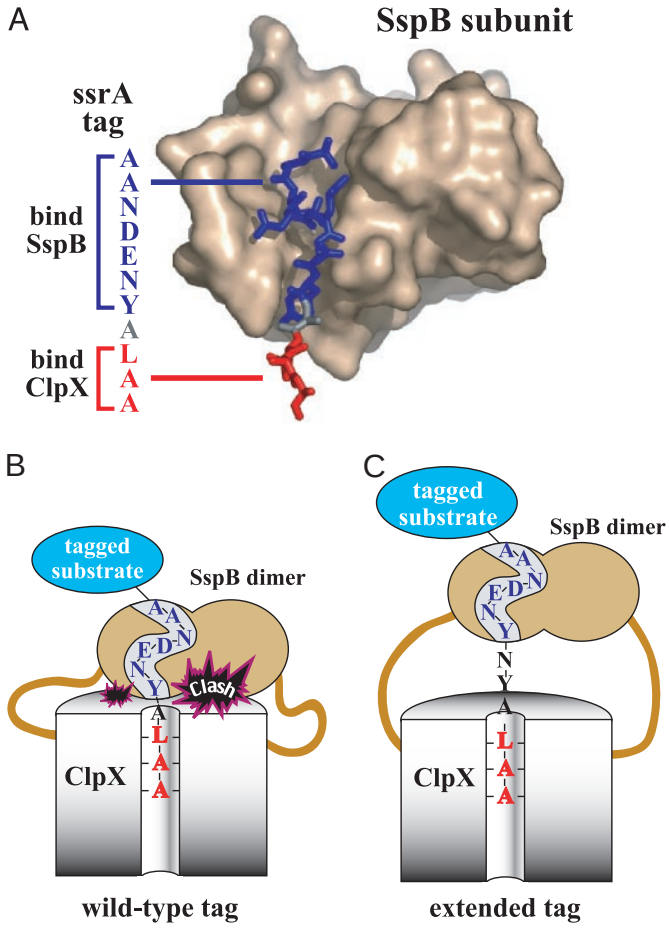

Fig. 1. SspB delivery of ssrA-tagged substrates to ClpXP. (*A*) Structure of SspB subunit with bound ssrA tag (14). SspB and ClpX contact residues in the blue and red portions of the ssrA tag, respectively (11). (*B*) Cartoon showing how SspB delivery of a substrate with a wild-type ssrA tag could result in a steric or electrostatic clash. (*C*) This clash could be relieved during delivery of a substrate with an extended ssrA tag in which the SspB- and ClpX-binding sites are farther apart.

Proteins and Peptides. An overexpression plasmid for GFP-ssrA (pMS30) was provided by J. Flynn (Massachusetts Institute of Technology; ref. 11). Plasmids GH7 (encoding GFP-ssrA^{NYNY}) and GH8 (encoding GFP-ssrA^{NYGSNY}) were constructed by replacing the cassette between the *Stu*I and *Hin*dIII restriction sites in the 3′ portion of the *gfp-ssrA* gene in pMS30. The presence of the expected mutations in the genes encoding GFP-ssrA^{NYNY} and GFP-ssrA^{NYGSNY} were confirmed by DNA sequencing. *Escherichia coli* ClpX, *E. coli* ClpP, GFP-ssrA, and variants, *E. coli* SspB-SBD (residues 1–117), and *E. coli* SspB were expressed and purified by published procedures (12, 16, 22, 27, 28). GFP-ssrA and variants were further purified on a MonoQ 10/10 column (Amersham Pharmacia Biosciences, Piscataway, NJ). The ssrA peptide (NH_2-NKKGRHGAANDENYALAA-COOH) and a derivative containing an N-terminal fluorescein were synthesized by the Massachusetts Institute of Technology Biopolymers Laboratory and purified on a Shimadzu LC-10AD-VP HPLC column. Concentrations were determined by UV absorbance at 280 nM, using extinction coefficients of 19,770 $M^{-1}\cdot cm^{-1}$ (GFP-ssrA and variants), 84,480 $M^{-1}\cdot cm^{-1}$ ($ClpX_6$), 125,160 $M^{-1}\cdot cm^{-1}$ ($ClpP_{14}$), 12,090 $M^{-1}\cdot cm^{-1}$ (SspB and SspB-SBD), and 1,280 $M^{-1}\cdot cm^{-1}$ (ssrA peptide). The concentration of fluorescent ssrA peptide was determined in basic ethanol (pH ≈10) by using an extinction coefficient at 500 nM of 92,300 $M^{-1}\cdot cm^{-1}$ (29). Note that concentrations of SspB are reported in monomer equivalents.

Activity and Binding Assays. Degradation assays were performed at 30°C as described (22). ClpXP degradation of GFP-ssrA or variants in PD buffer plus an ATP regeneration system was monitored by using a Photon Technology International (Lawrenceville, NJ) QM-2000-4SE spectrofluorometer (excitation at 467 nm, emission at 511 nm, and an 0.3-cm cuvette). Degradation rates were calculated from the initial linear loss of fluorescence. ClpXP-mediated degradation of [^{35}S]GFP-ssrA was assayed by the release of radioactive peptides soluble in ice-cold trichloroacetic acid (22). Curve fitting was performed by using KALEIDAGRAPH (Synergy Software, Reading, PA).

Binding of tagged GFP to SspB at 30°C was assayed by isothermal titration calorimetry, using a Microcal (Amherst, MA) VP-ITC calorimeter. After degassing, SspB (60 μM) was loaded into the 300-μl syringe and injected in 7.5-μl aliquots at 320-s intervals into a 1.4-ml cell containing 7 μM GFP-ssrA or GFP-ssrA^{NYNY}. Integration and least-squares fitting was performed by using ORIGIN (Microcal) software, after discarding the first data point. The absorbance spectrum of GFP-ssrA in the presence and absence of SspB was taken on an HP-8452a UV-Vis spectrophotometer.

The kinetics of ssrA peptide or GFP-ssrA binding to SspB at 30°C were assayed by changes in fluorescence (excitation at 467 nM and emission >495 nm) by using an Applied Photophysics (Surrey, U.K.) SX.18MV stopped-flow instrument. Stopped-flow samples were equilibrated at 30°C for 10 min before injection. Mixing ratios of 1:1 or 1:5 were used for association and dissociation experiments, respectively. For association assays, different amounts of SspB were used, and the concentrations, after mixing, of the fluorescent ssrA peptide or GFP-ssrA were 330 and 250 nM, respectively. For dissociation assays, SspB and fluorescent ssrA peptide were mixed (1 μM each) and diluted 6-fold into buffer containing 20 μM unlabeled peptide. For all stopped-flow experiments, at least 10 kinetic trajectories were collected, averaged, and fit to a single-exponential function by using Applied Photophysics software.

Results

Design of Extended-Spacing ssrA Tags. ClpX recognizes the three C-terminal residues of the 11-residue ssrA tag, whereas SspB contacts determinants in the seven N-terminal residues (ref. 11 and Fig. 1*A*). To move the ClpX- and SspB-binding sites farther apart, we designed an altered tag in which the NY sequence was repeated to generate a 13-residue variant (ssrA^{NYNY}) with the sequence AANDENYNYALAA. We also created a 15-residue tag (ssrA^{NYGSNY}) with the sequence AANDENYGSNYALAA. To ensure that the altered ssrA tags were functional, we fused them to the C terminus of GFP and determined K_m and V_{max} values for degradation by ClpXP (Table 1 and data not shown). The mutant tags caused only minor changes in these kinetic parameters, usually within experimental error, demonstrating that the mutations do not significantly alter tag interactions with ClpXP.

Improved SspB Delivery to ClpXP. To test whether the mutant tags improved SspB-mediated delivery to ClpXP, we measured degradation rates at different substrate concentrations in the presence of SspB. At saturating substrate concentrations, GFP-ssrA, GFP-ssrA^{NYNY}, and GFP-ssrA^{NYGSNY} were all degraded with comparable maximal velocities (Fig. 2*A* and Table 1). At low substrate concentrations, however, GFP-ssrA^{NYNY} (Fig. 2*A*) was degraded more efficiently than the wild-type substrate, as expected if the mutant tag reduced K_m for degradation. The K_m for SspB-mediated degradation of GFP-ssrA was calculated to be 75 nM, after correcting for the concentration of enzyme bound

BIOCHEMISTRY

Table 1. Constants for ClpXP degradation of ssrA-tagged molecules

Substrate	K_M, μM	V_{max}, $min^{-1}\cdot[ClpX_6]^{-1}$
GFP-ssrA*	1.1 ± 0.1	0.9 ± 0.1
NYNY*	0.8 ± 0.2	1.0 ± 0.1
NYGSNY*	1.0 ± 0.3	1.0 ± 0.2
GFP-ssrA†	75 ± 15	1.2 ± 0.1
NYNY†	20 ± 4	1.2 ± 0.1
NYGSNY†	15 ± 3	1.2 ± 0.1
GFP-ssrA‡	48 ± 4§	1.0§
NYNY‡	2.3 ± 0.5	1.0 ± 0.1
NYGSNY‡	3.0 ± 0.7	1.0 ± 0.1

*No SspB; 30°C; PD buffer.
†With [SspB] = [substrate]; 30°C; PD buffer.
‡With [SspB SBD] = 20 μM; 30°C; PD buffer.
§K_m value calculated by fitting with assumed V_{max} of 1.0 min^{-1}.

SspB·GFP-ssrA and for the concentration of GFP-ssrA not bound to SspB. However, K_m values for the extended-spacing substrates could not be determined from these experiments, because the concentrations of ClpXP·SspB·substrate and total SspB·substrate were too close to obtain a reliable value of the free SspB·substrate concentration.

To quantify differences in susceptibility to degradation, equal quantities of ^{35}S-GFP-ssrA and unlabeled GFP-ssrA^{NYNY} were mixed, and SspB-mediated degradation was assayed under conditions where the two substrates compete for ClpXP (Fig. 2*B*). The overall degradation rate (GFP-ssrA^{NYNY} plus GFP-ssrA) was determined by changes in fluorescence, and the degradation rate of [^{35}S]GFP-ssrA was determined by release of acid-soluble radioactivity, allowing calculation of the GFP-ssrA^{NYNY} degradation rate. Under these conditions, GFP-ssrA^{NYNY} was degraded ≈4-fold faster than GFP-ssrA (Fig. 2*B*), and GFP-ssrA^{NYGSNY} was degraded 5-fold faster (data not shown). Control experiments showed the same rate of ClpXP degradation of [^{35}S]GFP-ssrA assayed by fluorescence or acid-soluble radioactivity (Fig. 2*C*) and revealed similar rates of [^{35}S]GFP-ssrA and GFP-ssrA^{NYNY} degradation without SspB (Fig. 2*D*). When equal concentrations of two substrates compete for limiting enzyme, the ratio of V_{max}/K_m for processing of each substrate determines their relative degradation rates. This ratio allows calculation of K_m values of 15–20 nM for ClpXP degradation of SspB-bound GFP-ssrA^{NYNY} and GFP-ssrA^{NYGSNY} (Table 1). Thus, the K_m values observed for substrates bearing the mutant tags are substantially lower than the wild-type value. Because $K_m \approx K_d$ for ClpXP degradation of ssrA-tagged substrates (24), the extended-spacing ssrA tags must mediate stronger binding to the enzyme in ternary complexes with the SspB adaptor.

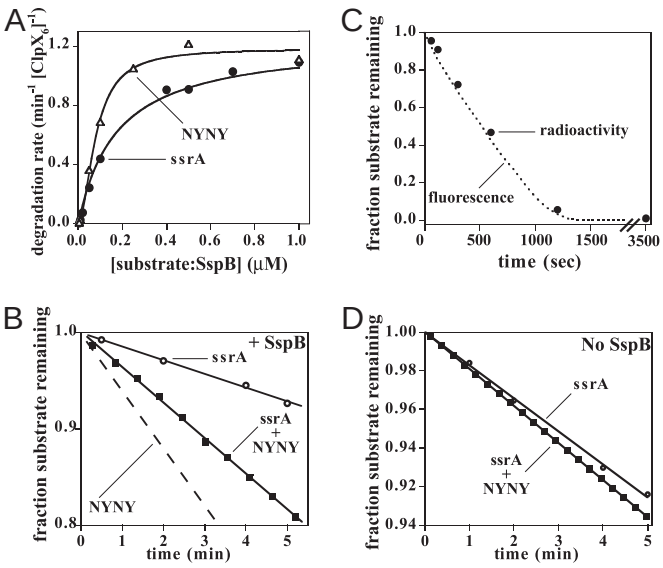

Fig. 2. ClpXP degradation of ssrA-tagged GFP variants in the presence of SspB. (*A*) Rates of degradation of tagged GFP in the presence of equimolar concentrations of SspB by ClpXP (50 nM $ClpX_6$ and 300 nM $ClpP_{14}$) were plotted as a function of substrate concentration. (*B*) [^{35}S]GFP-ssrA (2 μM) and GFP-ssrA^{NYNY} (2 μM) were degraded by ClpXP in the same reaction in the presence of SspB (4 μM). Degradation reactions were monitored by changes in fluorescence (total degradation) and by release of acid-soluble radioactive peptides from [^{35}S]GFP-ssrA. The degradation of GFP-ssrA^{NYNY} (dashed line) was calculated by subtracting the degradation of [^{35}S]GFP-ssrA from the total degradation. (*C*) Kinetics of degradation of [^{35}S]GFP-ssrA (2 μM) by ClpXP (100 nM $ClpX_6$ and 300 nM $ClpP_{14}$) in the presence of SspB (2 μM) were the same when monitored by loss of fluorescence (dotted line) or by release of acid-soluble radioactivity (●). (*D*) [^{35}S]GFP-ssrA (2 μM) and GFP-ssrA^{NYNY} (2 μM) were degraded by ClpXP in the same reaction in the absence of SspB. The rate of degradation of [^{35}S]GFP-ssrA (○) is only slightly slower than the combined rate of degradation of both proteins (■).

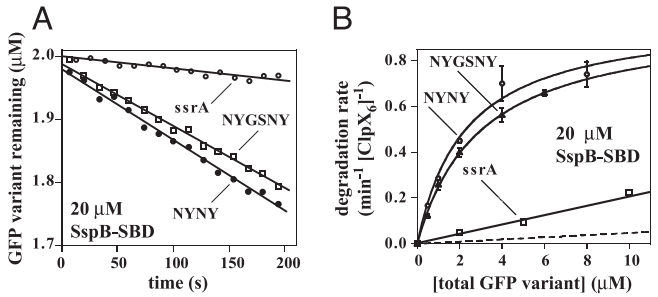

Fig. 3. ClpXP degrades the extended-tag substrates significantly faster than GFP-ssrA in the presence of the SBD of SspB. (*A*) Degradation of tagged GFP substrates (2 μM) by ClpXP (130 nM $ClpX_6$ and 300 nM $ClpP_{14}$) in the presence of the SspB SBD (20 μM). (*B*) Michaelis–Menten plots of degradation rates at different substrate concentrations in the presence of 20 μM SspB SBD (same conditions as *A*). The dashed line is the calculated contribution from free GFP-ssrA degradation (i.e., substrate not bound to the SspB SBD) by using K_d = 75 nM for SspB-SBD·GFP-ssrA binding, K_m = 1.1 μM, V_{max} = 0.9 $min^{-1}\cdot[ClpX_6]^{-1}$ (Table 1). Previous studies (16) show that SspB and its SBD bind ssrA-tagged substrates with essentially the same affinity. Kinetic parameters from Michaelis–Menten fits of the data are listed in Table 1. Because saturable kinetics were not observed for GFP-ssrA, the fit was constrained by assuming a V_{max} of 1 min^{-1}.

Reduced Conditional Inhibition. The isolated SBD of SspB inhibited ClpXP degradation of the extended-tag substrates less than degradation of GFP-ssrA (Fig. 3*A*). When substrate concentrations were varied in the presence of 20 μM SspB-SBD (Fig. 3*B*), ≈20-fold higher concentrations of GFP-ssrA ($K_m \approx 50$ μM) were required to attain the same rates of degradation observed for the extended-tag GFP substrates (K_m = 2–3 μM). Thus, moving the ClpX and SspB recognition determinants farther apart in the ssrA tag improves binding to ClpX in the presence of intact SspB or its SBD. The importance of the tethering interactions for both the wild-type and mutant substrates is illustrated by the fact that K_m values for ClpXP degradation are at least 100-fold lower in the presence of SspB than in the presence of its tethering-defective SBD.

Can GFP-ssrA bound to the isolated SspB SBD actually be degraded by ClpXP, or does the observed proteolysis result from degradation of adaptor-free substrate? The dashed line in Fig.

Table 2. Constants for SspB binding to ssrA-tagged molecules

Substrate	K_d, nM	ΔH, kcal/mol	k_{on}, $\mu M^{-1}\cdot s^{-1}$	k_{off}, s^{-1}
GFP-ssrA*	48 ± 9	20 ± 1	ND	ND
NYNY*	52 ± 11	17 ± 1	ND	ND
NYGSNY*	92 ± 18	22 ± 1	ND	ND
ssrA peptide*	650 ± 43†	ND	4.8 ± 0.1	3.1 ± 0.2
GFP-ssrA‡	75 ± 30	22 ± 1	4.6 ± 0.3	0.3 ± 0.1§
NYNY‡	ND	ND	4.4 ± 0.4	ND
NYGSNY‡	ND	ND	ND	ND
ssrA peptide‡	450 ± 14	ND	4.0 ± 0.1	1.8 ± 0.1

*At 30°C; buffer A.
†K_d value calculated as ratio of k_{off}/k_{on}.
‡At 30°C; PD buffer.
§k_{off} calculated as $K_d \cdot k_{on}$.

3*B* shows the calculated contribution of free GFP-ssrA to degradation observed in the presence of 20 μM SspB-SBD. Because the observed degradation is significantly higher than that expected from free substrate alone, we conclude that GFP-ssrA bound to the SspB-SBD is a substrate for ClpXP degradation.

Binding of Extended-Tag Substrates to SspB. To ensure that the mutations in the extended-spacing ssrA tags did not cause major changes in SspB interactions, isothermal titration calorimetry was used to assay binding (Table 2 and Fig. 4). SspB bound GFP-ssrA and the mutants with equilibrium dissociation constants of roughly 50–90 nM (30°C; buffer A or PD buffer). Hence, the extended-tag mutations do not significantly perturb equilibrium binding to SspB.

Dynamic Interactions Between SspB and ssrA Tags. Successful substrate delivery for degradation must involve dissociation of ssrA-tagged substrates from SspB because the tag and attached substrate are translocated through the ClpX pore and into ClpP. To determine whether tag dissociation might be a slow step in degradation, we used stopped-flow experiments to measure the kinetics of interactions between SspB and an ssrA peptide or ssrA-tagged GFP. Fig. 5*A* shows a time course, assayed by changes in fluorescence, for dissociation of an SspB complex with an ssrA peptide containing an N-terminal fluorescein. The rate constant for dissociation (k_{off}) was 3.1 s^{-1} (30°C; buffer A). Association also takes place in the subsecond time regime. Pseudo first-order rate constants (k_{obs}) for SspB-peptide association conditions were determined at different SspB concentrations and are plotted in Fig. 5*B*. The slope of this plot (4.8 $\mu M^{-1}\cdot s^{-1}$) is the association rate constant (k_{on}). Hence, both association and dissociation of the ssrA peptide and SspB occur rapidly. Similar rate constants for the SspB·ssrA–peptide interaction were obtained in PD buffer (Table 1). K_d values for SspB·peptide binding (450–650 nM), calculated from the kinetic constants, were similar to values determined directly for binding of the ssrA peptide to SspB or its SBD at a lower temperature (12, 16), but were ≈10-fold higher than K_d for the binding of SspB to GFP-ssrA (Table 2).

Studies of the kinetics of the SspB·GFP-ssrA interaction were facilitated by the finding that SspB binding causes spectral changes in the GFP chromophore, including appearance of an absorbance peak near 400 nm (Fig. 5*C*) and reduction in the fluorescence emission peak near 510 nm (data not shown). The CD spectrum of native GFP-ssrA was not altered upon SspB binding (data not shown), showing that GFP denaturation, which also results in an absorbance peak near 400 nM, is not the cause of the absorbance change. Assays of the kinetics of GFP-ssrA binding at different concentrations of SspB (Fig. 5*D*) yielded a

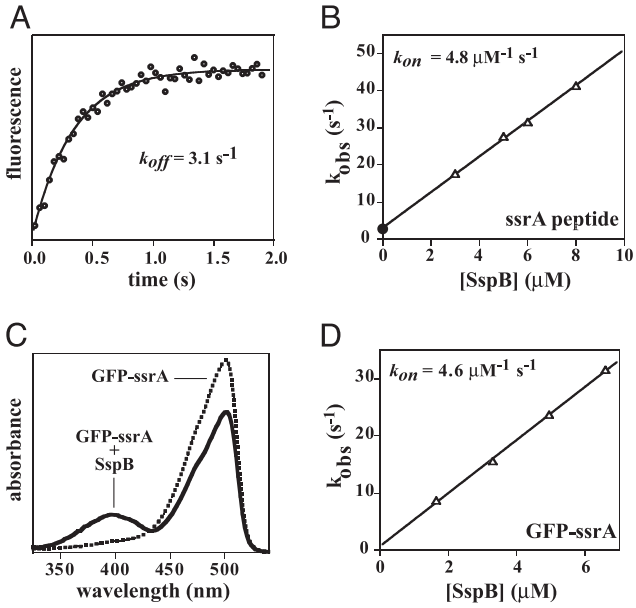

Fig. 5. Kinetics of dissociation and association of ssrA-tagged molecules with SspB. (*A*) Dissociation kinetics. SspB (1 μM) was prebound to an ssrA peptide with a N-terminal fluorescein (1 μM) and, at time 0, was diluted 6-fold into buffer containing excess unlabeled peptide (20 μM). The solid line is a single-exponential fit with a dissociation rate constant of 3.1 s^{-1}. (*B*) Association kinetics. The fluorescent ssrA peptide (330 nM) was mixed with different excess concentrations of SspB at time 0, first-order rate constants (k_{obs}) were determined by single-exponential fits of the kinetic trajectories. These rate constants (△) show a linear dependence on the total SspB concentration (R = 0.999), with a slope equal to the k_{on}. The y-intercept of the fit is very close to the k_{off} value (●), as expected for relaxation kinetics (39). (*C*) Absorbance spectra of GFP-ssrA (10 μM) in the presence (10 μM) or absence of SspB taken at room temperature in 10 mM Tris·HCl (pH 7.6). Under these conditions, SspB binding reduces the GFP-ssrA absorbance peak centered near 500 nM and results in a new peak ($\lambda_{max} \approx$ 400 nm). The intensity of this new peak was diminished in a hyperbolic fashion as the KCl concentration was raised (50% decrease at 16 mM KCl; data not shown). (*D*) GFP-ssrA (250 nM) was mixed with different concentrations of SspB and pseudo k_{obs} were determined by fits of kinetic trajectories measured by changes in fluorescence. The solid line is a linear fit (R = 0.999) with a slope of 4.6 $\mu M^{-1}\cdot s^{-1}$ and a y-intercept of 0.73 ± 0.5 s^{-1}.

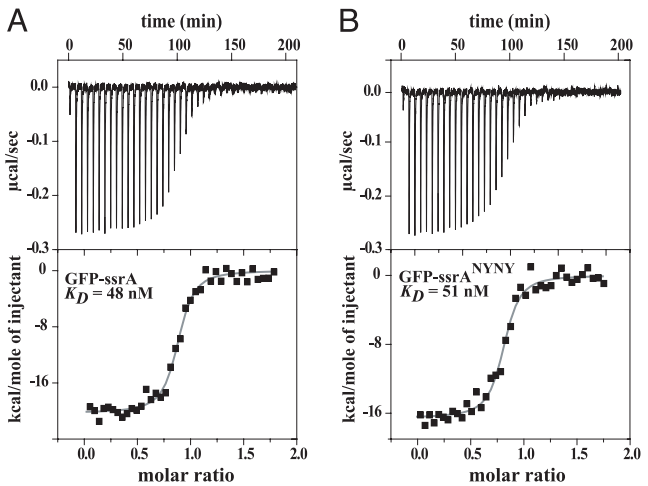

Fig. 4. Equilibrium binding of SspB to GFP-ssrA (*A*) or GFP-ssrA^{NYNY} (*B*) assayed by isothermal titration calorimetry at 30°C in buffer A. Thermodynamic parameters for these and additional binding experiments are listed in Table 2.

k_{on} of 4.6 $\mu M^{-1} \cdot s^{-1}$ (30°C; PD buffer). Dissociation could not be monitored directly because of hysteresis; changes in the environment of the GFP-ssrA chromophore apparently persist after dissociation of SspB. However, a dissociation rate constant of 0.3 s^{-1} was calculated from the k_{on} and equilibrium constant, indicating that the SspB·GFP-ssrA interaction is still highly dynamic with a half-life of ≈2 s. Because the maximal rate of SspB-mediated ClpXP degradation of GFP-ssrA is ≈1 min^{-1}, dissociation of GFP-ssrA from SspB does not appear to be a significant kinetic barrier in the overall degradation reaction.

Discussion

SspB enhances ClpXP degradation of ssrA-tagged substrates by helping to bring the substrate and enzyme together (6, 12), but it has not been clear whether all three sets of peptide–protein interactions (ClpX·SspB, SspB·ssrA, and ssrA·ClpX) all form simultaneously in a true ternary complex or whether only binary contacts (ClpX·SspB and SspB·ssrA) are made. In the former case, SspB would directly hand the ssrA-tagged substrate to ClpX, whereas the latter model would require substrate dissociation from SspB before engagement by ClpX. The results reported here support the direct-handoff model and suggest that ClpX and SspB can bind ssrA-tagged substrates concurrently, albeit with modest clashes that weaken the ternary interaction (Fig. 1*B*). As a consequence, efficient handoff only occurs in tethered delivery complexes where the local concentrations of the degradation tag and its docking site on ClpX are very high. This model explains why SspB binding conditionally inhibits ClpXP degradation of ssrA-tagged substrates when the tethering interactions between SspB and ClpX are blocked or removed (16).

The extended-spacing ssrA tags had little effect on degradation by ClpXP in the absence of SspB, but mediated improved binding and degradation when either SspB or its isolated SBD were present. These results support the idea that clashes between ClpX and SspB occur when these molecules bind concurrently to the wild-type ssrA tag but are relieved in the mutant tags because the ClpX and SspB binding sites are further apart (Fig. 1*C*). Concurrent binding of SspB and ClpX to the ssrA tag is required for direct handoff and is consistent with studies showing that complexes of SspB and ssrA-tagged substrates bind ClpX more tightly than either SspB or the substrates alone (12, 16, 18). Finally, we note that direct handoff is also supported by the finding that ClpXP degrades GFP-ssrA bound to the tethering defective SBD of SspB.

The extended-spacing degradation tags lower K_m for SspB-mediated ClpXP degradation by 4- to 5-fold relative to the wild-type ssrA tag, but they lower K_m in the presence of the SspB SBD by 16- to 20-fold (Table 1). Both results demonstrate improved ClpX interaction, and therefore are consistent with tag-dependent relief of unfavorable interactions between SspB and ClpX, but the effect is clearly larger in the context of the isolated SBD. The added sequences in extended tags may hinder binding to a small degree specifically in tethered complexes, whereas they relieve unfavorable interactions between SspB and ClpX in both tethered and untethered complexes.

To complete the process of substrate delivery, ssrA-tagged substrates must dissociate from SspB to allow full engagement and processing by ClpXP. We find that the complex of SspB with GFP-ssrA dissociates with a half-life of a few seconds in solution. This rate is much faster than the overall rate of SspB-mediated ClpXP degradation, and thus dissociation of the complex between SspB and the ssrA-tagged substrate should not limit the overall rate of degradation. Whether ClpX simply waits for spontaneous dissociation of the tagged substrate from SspB in ternary complexes or accelerates dissociation by pulling on the C-terminal end of the ssrA tag remains to be determined. The rapid dynamics of association and dissociation of the ssrA tag from SspB also ensures that the system equilibrates rapidly. Indeed, all of the peptide–protein interactions (ClpX·SspB, SspB·ssrA, and ssrA·ClpX) involved in SspB-mediated delivery of ssrA-tagged substrates to ClpXP are relatively weak and highly dynamic. The conformation of the ClpX machine must change during the ATPase cycle, which takes place on the subsecond time scale. Moreover, hydrolysis of hundreds of ATP molecules can be required for ClpXP to denature a single native substrate (22, 24, 30). The use of multiple weak and dynamic peptide–protein interactions presumably allows individual contacts to be broken easily but then to reform rapidly during the conformational excursions of the ATPase. This process may allow delivery complexes to remain intact for many cycles of ATP hydrolysis, whereas ClpX is attempting to denature native ssrA-tagged substrates.

Most of the energy for binding ssrA-tagged substrates to SspB comes from interactions between the tag and SspB, but GFP-ssrA binding was ≈10-fold tighter than ssrA-peptide binding to SspB. This difference could arise because native GFP makes a few favorable contacts with SspB (≈1 kcal/mol) or because the non-ssrA portions of the peptide make a few unfavorable contacts of the same magnitude. We favor the former model because the absorbance and fluorescence properties of GFP-ssrA are perturbed upon binding to SspB, indicating that there is, in fact, interaction between these two proteins. These spectral changes were more prominent at low ionic strength, which is consistent with the interaction having an electrostatic component. SspB binding may perturb the GFP chromophore, which is buried in the hydrophobic core (31), by stabilizing a slightly altered GFP conformation. Distinct equilibrium populations of GFP with spectral properties similar to those described here have been observed (32).

Evolution has not optimized the ssrA tag for maximal rates of SspB-mediated ClpXP degradation. Our results show that substrates bearing the extended-spacing mutant tags are degraded 4- to 5-fold faster than substrates with the wild-type tag under competitive conditions. Why has the efficiency of SspB-mediated ClpXP degradation of ssrA-tagged substrates not been maximized by natural selection? The design of the natural ssrA tag could be constrained because it must be added by the cotranslational machinery of the tmRNA system (25), or because it also serves as a degradation signal for other proteases (25, 33). There is, however, no significant support for either of these possibilities. We prefer the idea that SspB has important biological roles both as an enhancer and as an inhibitor of ClpXP degradation of ssrA-tagged substrates. Because SspB binding changes the wild-type ssrA tag from a "strong" to a "weak" degradation signal, ClpXP degradation of bound substrates depends on the tethering interactions. As a result, ClpXP degradation of complexes of SspB with ssrA-tagged substrates could be blocked in the cell by other substrates, adaptors, or regulatory proteins that prevented tethering of SspB to ClpX. Recent studies (34) have shown that the UmuD/D′ substrate competes with SspB for the tethering sites in the N-terminal domain of ClpX. Moreover, the RssB adaptor has been proposed to interact with ClpX in a manner similar to SspB (17).

Interestingly, *E. coli* has many ways to prevent or slow degradation of ssrA-tagged substrates that arise from aberrant translation and therefore represent a form of intracellular debris. For example, both SspB and the ClpS adaptor inhibit ClpAP degradation of ssrA-tagged substrates (10, 11). Why would a cell add a very efficient degradation tag to proteins it wants to degrade and then repress proteolysis of these same polypeptides? Because the number of ClpXP and ClpAP proteases are limited in the cell (≈100 copies each; ref. 35), these enzymes may be easily saturated when substrates are abundant. Under such conditions, delaying proteolysis of ssrA-tagged proteins could allow ClpAP and ClpXP to degrade more critical substrates such

as key transcription factors, including stress regulators. The inhibitory activities of SspB could be especially important under adverse conditions, where translational mistakes and the level of ssrA tagging were high, and ClpAP or ClpXP degradation of specific substrates was needed for an efficient stress response. Indeed, the main function of proteolytic adapters may be to prioritize the proteolysis of different substrates under conditions where the degradation capacity of the cell is stressed.

The RssB adaptor, which delivers σ^S for ClpXP degradation, also functions as an inhibitor of σ^S function under some conditions (7, 36–38). Becker *et al.* (38) have speculated that the inhibition function of adaptors may have evolved before their recruitment as enhancers of protein degradation. Thus, SspB may initially have functioned largely as a degradation inhibitor. This proposal is consistent with the obstruct-then-stimulate mechanism, which SspB uses for delivery of ssrA-tagged substrates to ClpXP, and with the fact that SspB inhibits ClpAP degradation of ssrA-tagged substrates (11). Can inhibitors be turned into enhancers by tethering the inhibition complex to an appropriate protease? Inhibition of ClpAP degradation has been ascribed to overlap between ClpA- and SspB-binding determinants in the ssrA tag (11). Because ClpA does not contain tethering sites for SspB, any clash that substantially weakened concurrent ClpA and SspB binding to the tag would obviously be inhibitory in a manner analogous to inhibition of ClpXP degradation by tethering-defective SspB. In this regard, however, it would be interesting to determine whether SspB could deliver substrates to ClpA variants bearing the ClpX N-domain, which contains the tethering sites for SspB.

We thank David Wah, Julia Flynn, and other members of the Sauer and Baker laboratories for materials and advice, and the Multiuser Facility for the Study of Complex Molecular Systems (National Science Foundation Grant 0070319) for the use of equipment. This work was supported by National Institutes of Health Grant AI-16892. T.A.B. is an employee of Howard Hughes Medical Institute.

1. Gottesman, S. (1996) *Annu. Rev. Genet.* **30,** 465–506.
2. Gottesman, S., Wickner, S. & Maurizi, M. R. (1997) *Genes Dev.* **11,** 815–823.
3. Gottesman, S., Maurizi, M. R. & Wickner, S. (1997) *Cell* **91,** 435–438.
4. Pickart, C. M. & Cohen, R. E. (2004) *Nat. Rev. Mol. Cell Biol.* **5,** 177–187.
5. Kondo, H., Rabouille, C., Newman, R., Levine, T. P., Pappin, D., Freemont, P. & Warren, G. (1997) *Nature* **388,** 75–78.
6. Levchenko, I., Seidel, M., Sauer, R. T. & Baker, T. A. (2000) *Science* **289,** 2354–2356.
7. Zhou, Y., Gottesman, S., Hoskins, J. R., Maurizi, M. R. & Wickner, S. (2001) *Genes Dev.* **15,** 627–637.
8. Schlothauer, T., Mogk, A., Dougan, D. A., Bukau, B. & Turgay, K. (2003) *Proc. Natl. Acad. Sci. USA* **100,** 2306–2311.
9. Dougan, D. A., Mogk, A., Zeth, K., Turgay, K. & Bukau, B. (2002) *FEBS Lett.* **529,** 6–10.
10. Dougan, D. A., Reid, B. G., Horwich, A. L. & Bukau, B. (2002) *Mol. Cell* **9,** 673–683.
11. Flynn, J. M., Levchenko, I., Seidel, M., Wickner, S. H., Sauer, R. T. & Baker, T. A. (2001) *Proc. Natl. Acad. Sci. USA* **98,** 10584–10589.
12. Wah, D. A., Levchenko, I., Baker, T. A. & Sauer, R. T. (2002) *Chem. Biol.* **9,** 1237–1245.
13. Song, H. K. & Eck, M. J. (2003) *Mol. Cell* **12,** 75–86.
14. Levchenko, I., Grant, R. A., Wah, D. A., Sauer, R. T. & Baker, T. A. (2003) *Mol. Cell* **12,** 365–372.
15. Wojtyra, U. A., Thibault, G., Tuite, A. & Houry, W. A. (2003) *J. Biol. Chem.* **278,** 48981–48990.
16. Wah, D. A., Levchenko, I., Rieckhof, G. E., Bolon, D. N., Baker, T. A. & Sauer, R. T. (2003) *Mol. Cell* **12,** 355–363.
17. Dougan, D. A., Weber-Ban, E. & Bukau, B. (2003) *Mol. Cell* **12,** 373–380.
18. Bolon, D. N., Wah, D. A., Hersch, G. L., Baker, T. A. & Sauer, R. T. (2004) *Mol. Cell* **13,** 443–449.
19. Gottesman, S., Clark, W. P., de Crecy-Lagard, V. & Maurizi, M. R. (1993) *J. Biol. Chem.* **268,** 22618–22626.
20. Wojtkowiak, D., Georgopoulos, C. & Zylicz, M. (1993) *J. Biol. Chem.* **268,** 22609–22617.
21. Wawrzynow, A., Wojtkowiak, D., Marszalek, J., Banecki, B., Jonsen, M., Graves, B., Georgopoulos, C. & Zylicz, M. (1995) *EMBO J.* **14,** 1867–1877.
22. Kim, Y. I., Burton, R. E., Burton, B. M., Sauer, R. T. & Baker, T. A. (2000) *Mol. Cell* **5,** 639–648.
23. Burton, R. E., Baker, T. A. & Sauer, R. T. (2003) *Protein Sci.* **12,** 893–902.
24. Kenniston, J. A., Baker, T. A., Fernandez, J. M. & Sauer, R. T. (2003) *Cell* **114,** 511–520.
25. Keiler, K. C., Waller, P. R. & Sauer, R. T. (1996) *Science* **271,** 990–993.
26. Gottesman, S., Roche, E., Zhou, Y. & Sauer, R. T. (1998) *Genes Dev.* **12,** 1338–1347.
27. Levchenko, I., Yamauchi, M. & Baker, T. A. (1997) *Genes Dev.* **11,** 1561–1572.
28. Yakhnin, A. V., Vinokurov, L. M., Surin, A. K. & Alakhov, Y. B. (1998) *Protein Expression Purif.* **14,** 382–386.
29. Seybold, P. G., Gouterman, M. & Callis, J. (1969) *Photochem. Photobiol.* **9,** 229–242.
30. Burton, R. E., Siddiqui, S. M., Kim, Y. I., Baker, T. A. & Sauer, R. T. (2001) *EMBO J.* **20,** 3092–3100.
31. Ormo, M., Cubitt, A. B., Kallio, K., Gross, L. A., Tsien, R. Y. & Remington, S. J. (1996) *Science* **273,** 1392–1395.
32. Chattoraj, M., King, B. A., Bublitz, G. U. & Boxer, S. G. (1996) *Proc. Natl. Acad. Sci. USA* **93,** 8362–8367.
33. Herman, C., Thevenet, D., Bouloc, P., Walker, G. C. & D'Ari, R. (1998) *Genes Dev.* **12,** 1348–1355.
34. Neher, S. B., Sauer, R. T. & Baker, T. A. (2003) *Proc. Natl. Acad. Sci. USA* **100,** 13219–13224.
35. Ortega, J., Lee, H. S., Maurizi, M. R. & Steven, A. C. (2004) *J. Struct. Biol.* **146,** 217–226.
36. Zhou, Y. & Gottesman, S. (1998) *J. Bacteriol.* **180,** 1154–1158.
37. Becker, G., Klauck, E. & Hengge-Aronis, R. (1999) *Proc. Natl. Acad. Sci. USA* **96,** 6439–6444.
38. Becker, G., Klauck, E. & Hengge-Aronis, R. (2000) *Mol. Microbiol.* **35,** 657–666.
39. Fersht, A. (1985) *Enzyme Structure and Mechanism* (Freeman, New York).